



南京大學
Nanjing University

Nuclear Symmetry Energy Constrained by Cluster Radioactivity

Chang Xu (许昌)

Department of Physics, Nanjing University

2016.6.13-18@NuSym2016

Outline

1. Cluster radioactivity: brief review and our recent microscopic calculations.....

Collaborators: Z. Ren, G. Roepke, P. Schuck, H. Horiuchi, A. Tohsaki, T. Yamada, Y. Funaki, B. Zhou

2. Symmetry energy: the HVH theorem, optical potential, analytical formulas for symmetry energy.....

Collaborators: Bao-An Li, Lie-Wen Chen, Che-Ming Ko

3. Attempt to extract symmetry energy from cluster radioactivity data

4. Short summary

1. Cluster radioactivity

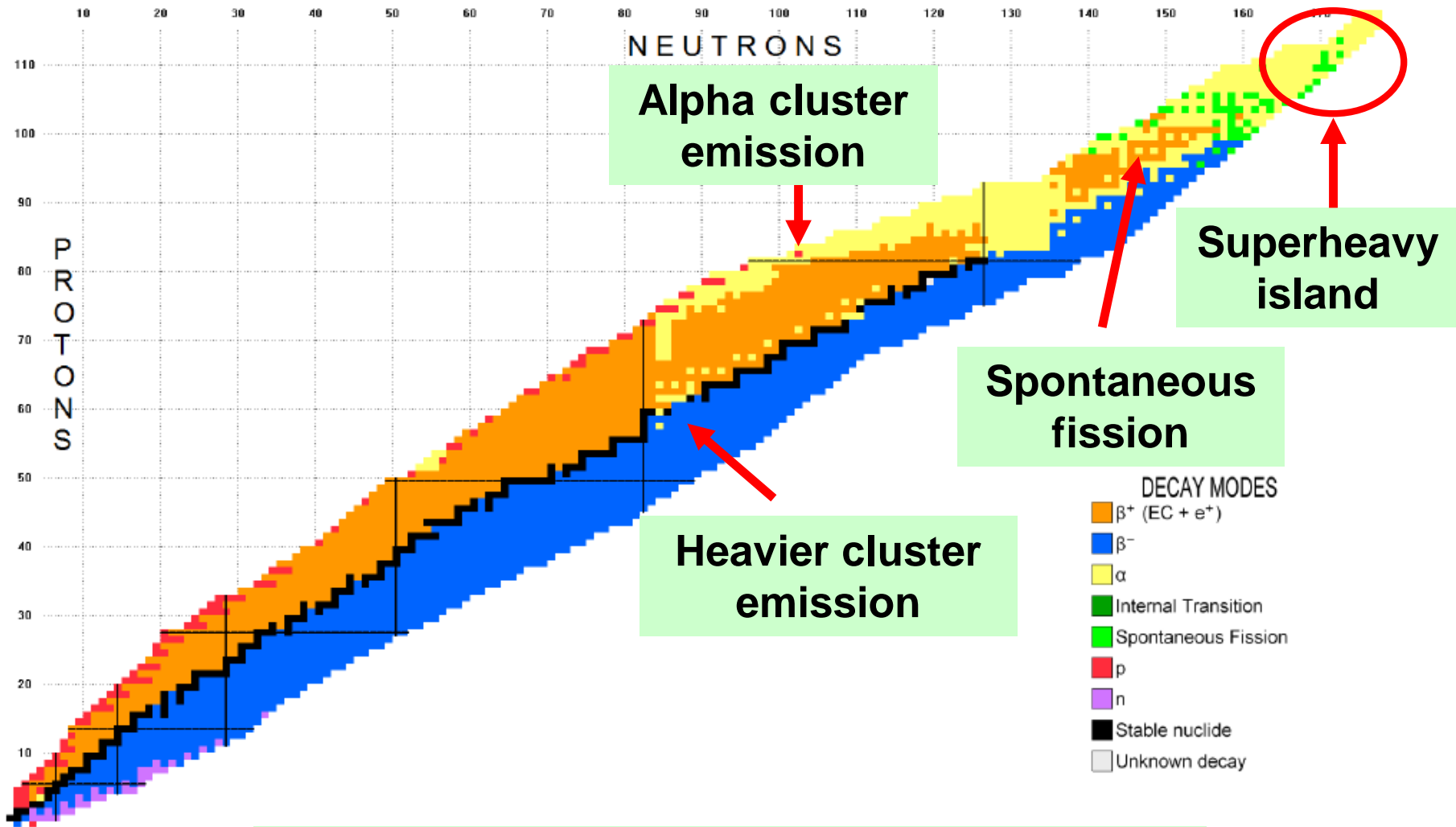


Chart of Nuclides

Importance of cluster radioactivity

- **Alpha decay/cluster radioactivity: an old problem but renewed interest in recent years**
- **Superheavy nuclei**
- **Nuclear properties: energy, lifetime, and nuclear spin and parity, nuclear interactions, deformation, clustering effect, shell effect....**
- **Phenomenological Formulas:**
- **The Geiger-Nuttall law, Viola-Seaborg formula , Other forms of decay formulas**
- **Theoretical Approaches :**
- **Shell model , Cluster model, Fission-like model, A mixture of shell and cluster model configurations....**

Decay theory in textbooks

p_α , ν , and \mathcal{T}

- (1) Preformation probability
- (2) Frequency (Pre-exponential factor)
- (3) Exponential factor

Energy and mass dependence. Using p_α , ν , and \mathcal{T} obtained above, we can write the transition probability as

$$\mathcal{W} = p_\alpha \nu \mathcal{T}$$

To put this expression into a form so that it can be compared with the Geiger-Nuttall law of Eq. (4-61), we take the logarithm in the base 10 for both sides and obtain the result

$$\begin{aligned} \log_{10} \mathcal{W} &= \log_{10} p_\alpha + \log_{10} \nu + \log_{10} \mathcal{T} \\ &= 20.46 + \log_{10} \frac{\sqrt{E_\alpha}}{A^{1/3}} + 1.42 \sqrt{Z A^{1/3}} - 1.72 \frac{Z}{\sqrt{E_\alpha}} \end{aligned} \quad (4-65)$$

The dominant energy dependence comes from the last term, in agreement with the empirical result of the Geiger-Nuttall law.

Decay theory in textbooks

(1) Preformation probability (most difficult)

The probability W for α -particle emission from a heavy nucleus by tunneling may be separated into a product of three factors. The first is the probability p_α to find an α -particle inside the nucleus. In a heavy nucleus, there is a good chance for two protons and two neutrons to form an α -like entity. We shall call such an object an α -cluster. However, this is only one of the many possible components of the wave function for such a nucleus. As a result, it is not easy to make an estimate for the value of p_α . A crude way is to say that it must be essentially of the same order of magnitude for all heavy nuclei, as there are only small fractional differences in their masses and we shall take $p_\alpha \sim 0.1$ as a rough guide.

This is not true for shell region nuclei!

Decay theory in textbooks

(2) Frequency (Pre-exponential factor)

Once an α -cluster is formed inside the nucleus, it must come to the surface before it can tunnel through the barrier. The frequency ν with which it appears at the edge of the potential well depends on the velocity v it travels and the size of the potential well. A reasonable way to estimate ν is to take the well size as twice the nuclear radius R . With this assumption we obtain the result,

$$\nu = \frac{v}{2R} = \frac{\sqrt{2K/M_\alpha}}{2R}$$

where K is the kinetic energy of the α -cluster inside the well and M_α its mass. The precise value of K depends on the depth of the potential well and is not well known.

$E_\alpha = 5.6$ MeV. It is about an order of magnitude larger than the best values deduced from measurements. Part of the reason for the poor agreement comes from the fact that heavy nuclei do not have the simple spherical shape assumed here. Furthermore, the replacement of K by E_α may also have cost some loss of accuracy.

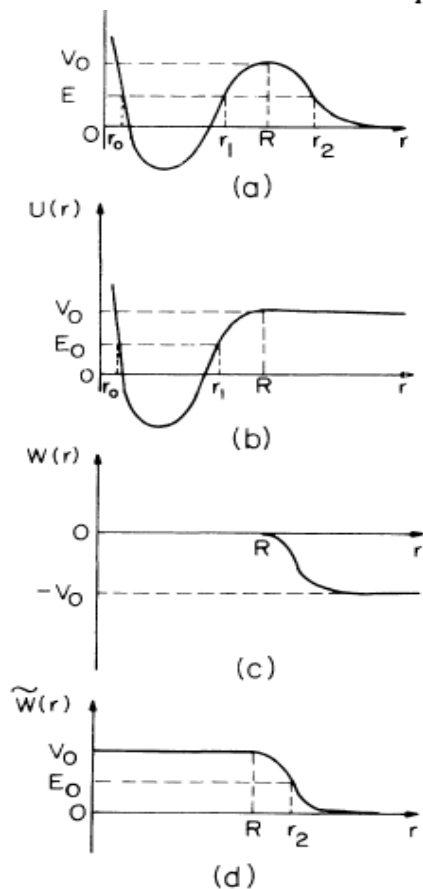
Decay Width and Shift of a Quasistationary State

S. A. Gurvitz

Weizmann Institute of Science, 76 100 Rehovot, Israel

and

G. Kalbermann

The Hebrew University of Jerusalem, 91 904 Jerusalem, Israel**A. Exact results**

Consider a potential barrier of any shape, a typical example of which is shown in Fig. 1. We split this potential into two parts $V(r) = U(r) + W(r)$ as shown in Fig. 2 such that $U(r) = V(r)$ for $r \leq R$, $U(r) = V(R) = V_0$ for $r > R$, and $W(r) = 0$ for $r \leq R$, $W(r) = V(r) - V_0$ for $r > R$.

Consider the state $|\Phi_0\rangle$ which is an eigenstate of the Hamiltonian $H_0 = -\hbar^2(\nabla^2/2m) + U(r)$ with an eigenvalue E_0 where $E_0 < V_0$ [Fig. 2(a)]. The state $|\Phi_0\rangle$ is the "unperturbed" bound state, and the perturbation $W(r)$ transforms it to a quasistationary one. We switch on the "distorting" potential $W(r)$ at $t=0$. Then the state

Here χ_k is the regular at the origin and $\chi_k^{(+)}$ is the irregular (outgoing) eigenstate of the Hamiltonian $-(\hbar^2\nabla^2/2m) + \tilde{W}(r)$, with the asymptotic behaviors

$$N = \left[\int_{r_0}^{r_1} \frac{1}{p(r)} \cos^2 \left[\int_{r_0}^r p(r') dr' - \frac{\pi}{4} \right] dr \right]^{-1}. \quad (3.7)$$

If the contribution from the classically forbidden regions is not small, these regions should also be taken into account in Eq. (3.7). Substituting Eq. (3.6) into Eqs. (3.3) and (3.4) we obtain for the quasiclassical width and shift

$$\Gamma = \frac{\hbar^2 N}{4m} \exp \left[-2 \int_{r_1}^{r_2} |p(r)| dr \right], \quad (3.8)$$

For the high-lying states where $\varphi_0(r)$ oscillates strongly, one can replace the cosine term in Eq. (3.7) by $\frac{1}{2}$. Then

$$N^{-1} = \frac{1}{2m} \int_{r_0}^{r_1} \frac{m}{p(r)} dr = \frac{T\hbar}{4m}, \quad (3.10)$$

where T is the classical period of motion. Substituting Eq. (3.10) into Eq. (3.8) we obtain the famous Gamow formula for the width of the quasistationary state with preexponential Gamow factor \hbar/T . However, our pre-factor factor $N\hbar^2/4$ in Eq. (3.8) is more general and can also be used as soon as the quasiclassical approximation is applicable to the bound-state wave function in a classically forbidden region, which is correct even for low-lying bound states.

Frequency

Vs

Well defined

pre-factor

Decay theory in textbooks

(3) Exponential factor

to calculate. In this limit, $\kappa b \rightarrow \infty$, and $\sinh \kappa b \rightarrow e^{\kappa b}$. The transmission coefficient in Eq. (4-62) simplifies to the form

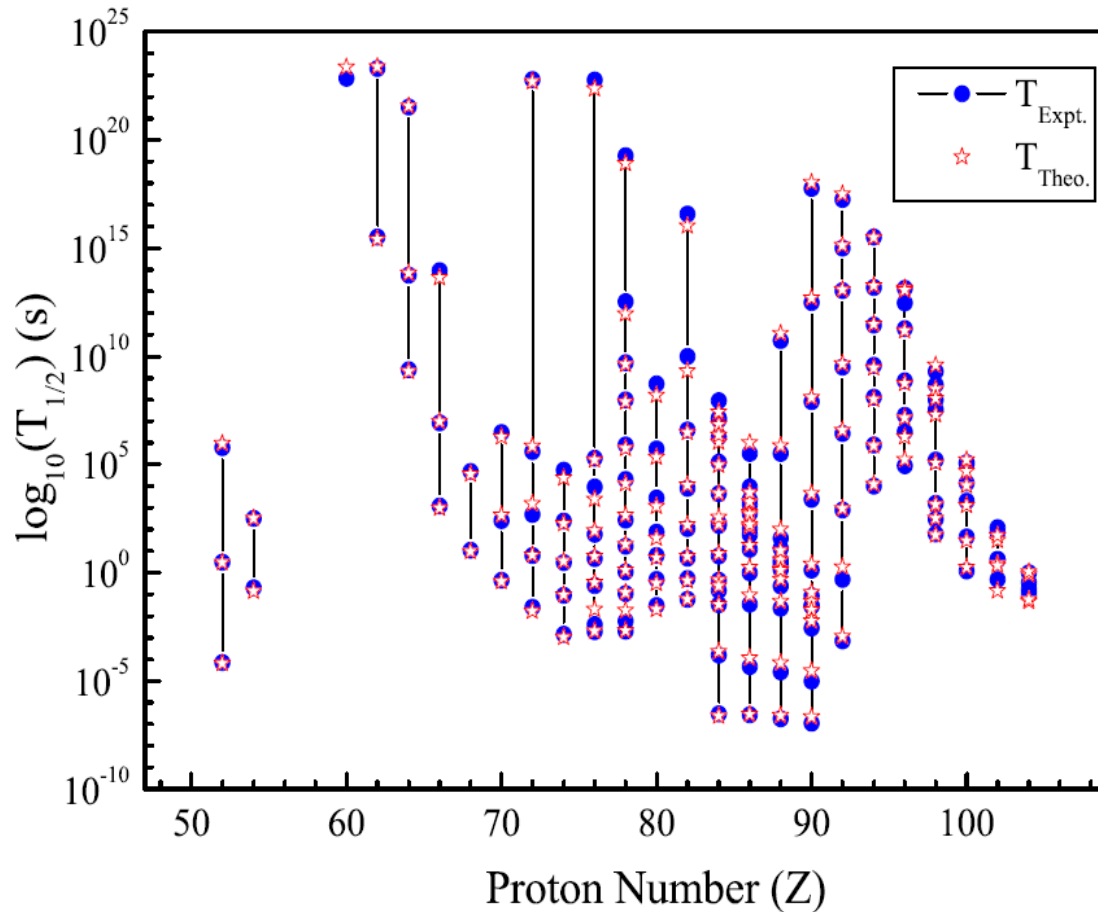
$$\mathcal{T} \rightarrow e^{-2\kappa b} \quad (4-63)$$

The factor $e^{-\kappa b}$ expresses the attenuation of the amplitude of the wave in going through the barrier, and it is quite reasonable to expect that the transmission coefficient is essentially given by the square of this factor. For our case of $V_0 \approx 30$ MeV and E_α in

The form of the solution, however, remains very similar to that given in Eq. (4-63) if we make the replacement

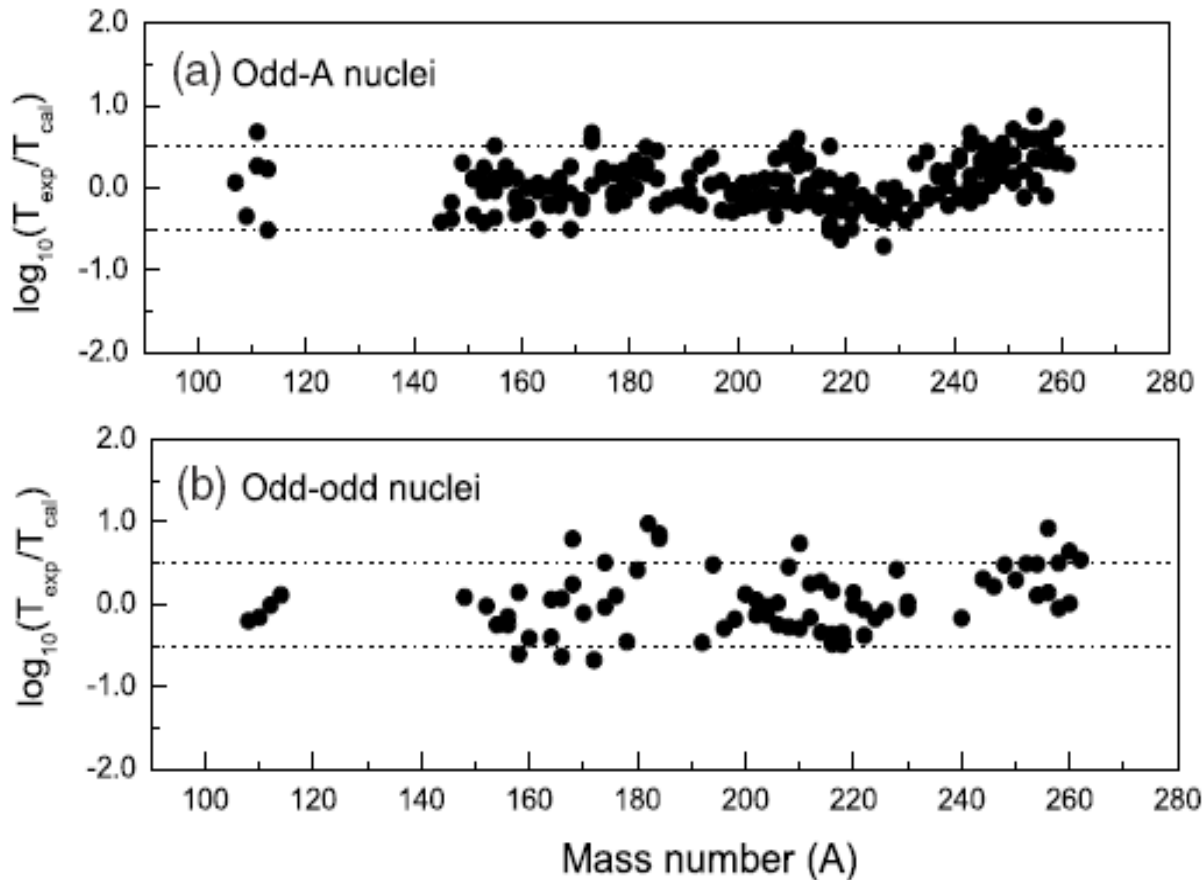
$$\kappa b \rightarrow \int_R^{R_1} \sqrt{\frac{2\mu}{\hbar^2} \{V_b(r) - E_\alpha\}}^{1/2} dr$$

Alpha-decay half-lives of even-even nuclei of ground-state transitions (Z=52-104)

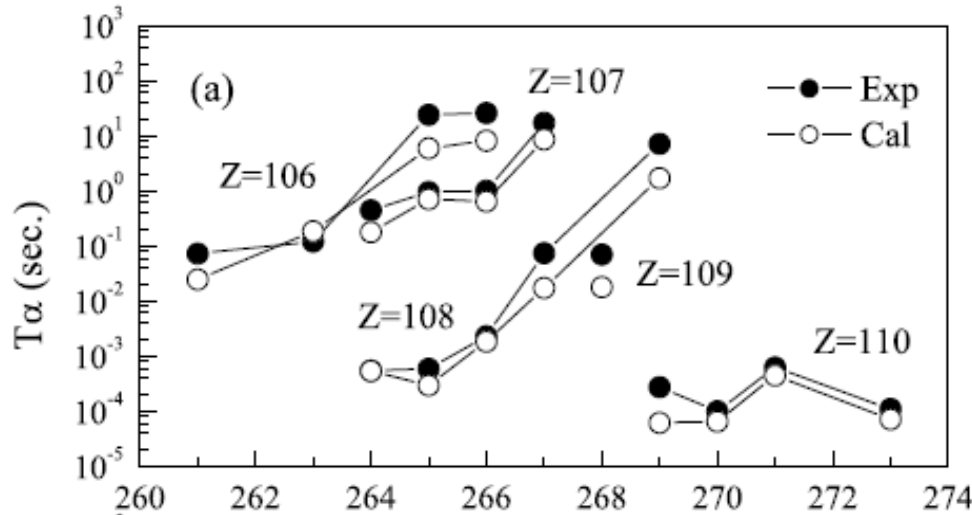


Circles : Experiment
Stars : Theory

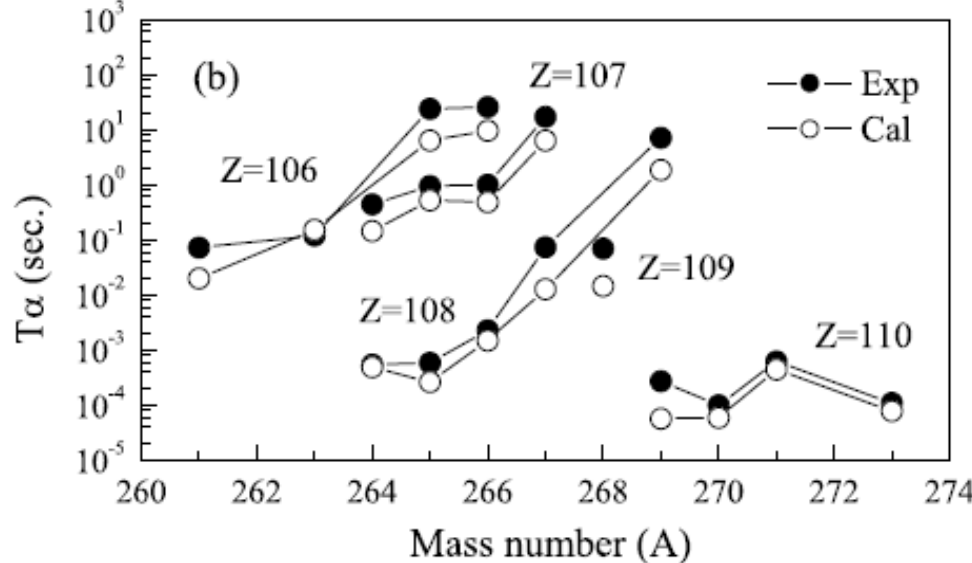
The factor of agreement for odd nuclei of ground-state transitions (Z=52-105)



The experimental and calculated alpha-decay half-lives of nuclei with $Z=106-110$



Deformation: the macroscopic-microscopic model (MM)



Deformation: the relativistic mean-field model (RMF) with a TMA force parameter

TABLE I. Comparison of average and rms deviations of DDCM and GLDM.

| Nuclide | Number | Average deviation | rms deviation |
|-----------|-----------|-------------------|------------------|
| Even-even | 157 (131) | 0.209 | 0.267(0.35) |
| Odd-A | 231 (192) | 0.229 | 0.285(0.57/0.71) |
| Odd-odd | 79 (50) | 0.318 | 0.435(0.99) |

A constant alpha preformation factor is OK for open shell nuclei, but not for shell region nuclei!

**How to calculate the preformation factor microscopically?
(three quantities self-consistently)**

One must first test the theory for alpha decay of ^{212}Po

α -decay width of ^{212}Po from a quartetting wave function approach

Chang Xu,^{1,*} Zhongzhou Ren,^{1,2,†} G. Röpke,^{3,‡} P. Schuck,^{4,5,§} Y. Funaki,⁶ H. Horiuchi,^{7,8} A. Tohsaki,⁷ T. Yamada,⁹ and Bo Zhou¹⁰

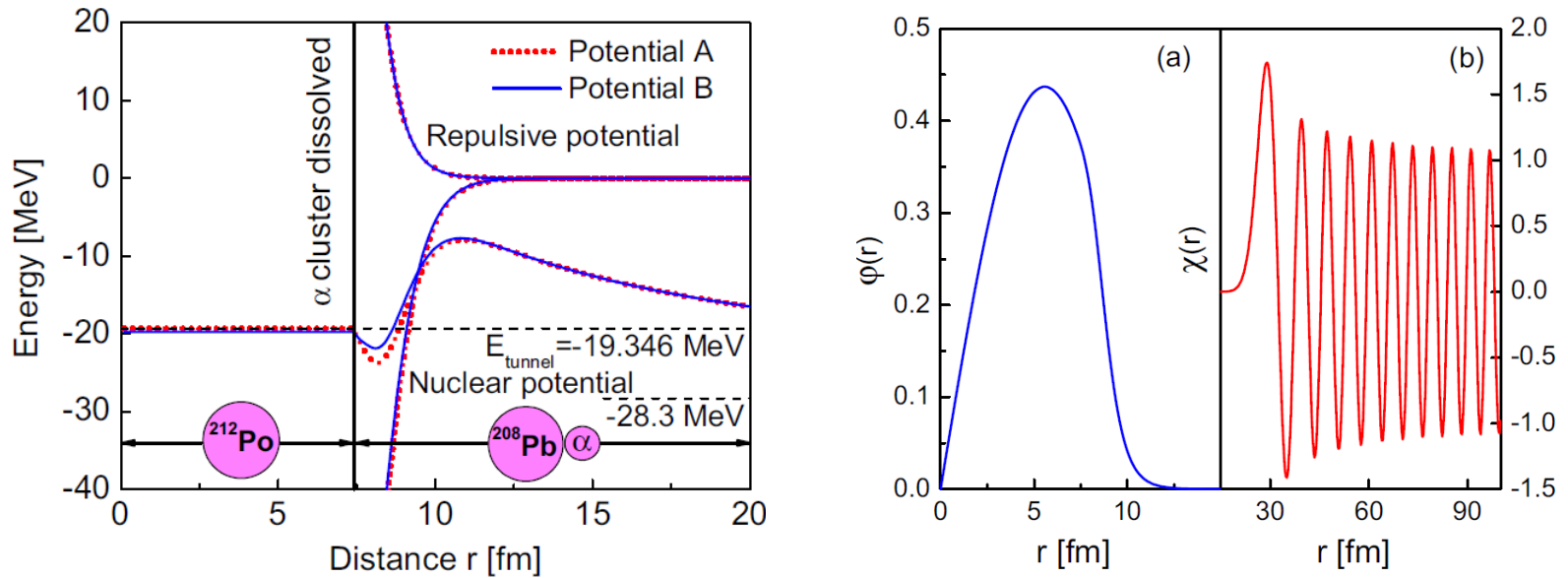


TABLE I. The calculated preformation probability and decay half-life of ^{212}Po using different sets of effective c.m. potentials.

| Potential | c (MeV fm) | d (MeV fm) | E_{tunnel} (MeV) | Fermi energy μ_4 (MeV) | $E_{\text{tunnel}} - \mu_4$ (MeV) | Preform. factor P_α | Decay half-life $T_{1/2}$ (s) |
|-----------|-----------------|-----------------|------------------------------|-------------------------------|--------------------------------------|-------------------------------|----------------------------------|
| A | 13866.30 | 4090.51 | -19.346 | -19.346 | 0 | 0.367 | 2.91×10^{-8} |
| B | 11032.08 | 3415.56 | -19.346 | -19.771 | 0.425 | 0.142 | 2.99×10^{-7} |



Strong
correlation

Measured
data

Symmetry Energy

| Decay | Q (MeV) | $\log_{10} T_{1/2}^{\text{expt}}$ (s) |
|--|-----------|---------------------------------------|
| $^{221}\text{Fr} - ^{207}\text{Tl} + ^{14}\text{C}$ | 31.29 | 14.52 |
| $^{221}\text{Ra} - ^{207}\text{Pb} + ^{14}\text{C}$ | 32.40 | 13.37 |
| $^{222}\text{Ra} - ^{208}\text{Pb} + ^{14}\text{C}$ | 33.05 | 11.10 |
| $^{223}\text{Ra} - ^{209}\text{Pb} + ^{14}\text{C}$ | 31.83 | 15.05 |
| $^{224}\text{Ra} - ^{210}\text{Pb} + ^{14}\text{C}$ | 30.54 | 15.90 |
| $^{226}\text{Ra} - ^{212}\text{Pb} + ^{14}\text{C}$ | 28.20 | 21.29 |
| $^{228}\text{Th} - ^{208}\text{Pb} + ^{20}\text{O}$ | 44.72 | 20.73 |
| $^{230}\text{Th} - ^{206}\text{Hg} + ^{24}\text{Ne}$ | 57.76 | 24.63 |
| $^{231}\text{Pa} - ^{207}\text{Tl} + ^{24}\text{Ne}$ | 60.41 | 22.89 |
| $^{232}\text{U} - ^{208}\text{Pb} + ^{24}\text{Ne}$ | 62.31 | 20.39 |
| $^{233}\text{U} - ^{209}\text{Pb} + ^{24}\text{Ne}$ | 60.49 | 24.84 |
| $^{234}\text{U} - ^{206}\text{Hg} + ^{28}\text{Mg}$ | 74.11 | 25.74 |
| $^{236}\text{Pu} - ^{208}\text{Pb} + ^{28}\text{Mg}$ | 79.67 | 21.65 |
| $^{238}\text{Pu} - ^{206}\text{Hg} + ^{32}\text{Si}$ | 91.19 | 25.30 |
| $^{242}\text{Cm} - ^{208}\text{Pb} + ^{34}\text{Si}$ | 96.51 | 23.11 |

2. Symmetry energy

The density dependence of nuclear symmetry energy
----an important issue in both **nuclear physics** and **astrophysics**

The diagram illustrates the equation for the energy per nucleon in asymmetric nuclear matter, $E(\rho_n, \rho_p)$. The equation is presented as $E(\rho_n, \rho_p) = E_0(\rho_n = \rho_p) + E_{sym}(\rho) \left(\frac{\rho_n - \rho_p}{\rho} \right)^2 + o(\delta^4)$. Annotations include: a pink arrow pointing from 'symmetry energy' to $E_{sym}(\rho)$; a red arrow pointing from 'Isospin asymmetry' to the fraction $\frac{\rho_n - \rho_p}{\rho}$; a blue arrow pointing from 'Energy per nucleon in symmetric nuclear matter' to $E_0(\rho_n = \rho_p)$; and a black arrow pointing from 'Energy per nucleon in asymmetric nuclear matter' to the entire equation.

$$E(\rho_n, \rho_p) = E_0(\rho_n = \rho_p) + E_{sym}(\rho) \left(\frac{\rho_n - \rho_p}{\rho} \right)^2 + o(\delta^4)$$

symmetry energy

Isospin asymmetry

Energy per nucleon in symmetric nuclear matter

Energy per nucleon in asymmetric nuclear matter

Questions:

- *Is there a general principle at some level, independent of the interaction and many-body theory, telling us what determines the symmetry energy and its slope?*
- *Is there direct way to determine the symmetry energy and its slope at saturation density?*
- *Why the symmetry energy at high-density is so uncertain?*

Hugenholtz, N. M.
Van Hove, L.
1958

Physica XXIV
363–376

The HVH theorem

A THEOREM ON THE SINGLE PARTICLE ENERGY IN A FERMI GAS WITH INTERACTION

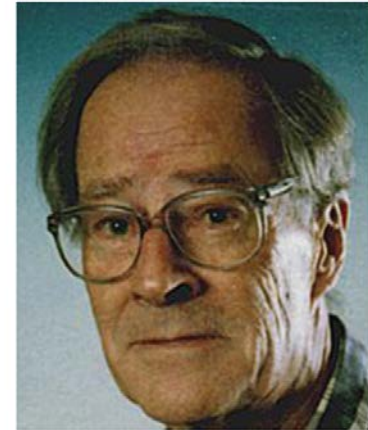
by N. M. HUGENHOLTZ and L. VAN HOVE

Instituut voor theoretische fysica der Rijksuniversiteit, Utrecht, Nederland

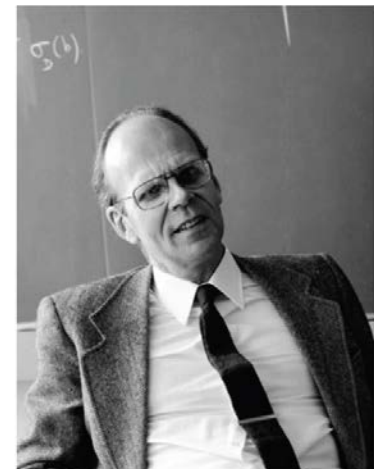
Synopsis

This paper investigates single particle properties in a Fermi gas with interaction at the absolute zero of temperature. In such a system a single particle energy has only a meaning for particles of momentum $|k|$ close to the Fermi momentum k_F . These single particle states are metastable with a life-time approaching infinity in the limit $|k| \rightarrow k_F$. The limiting value of the energy is called the Fermi energy E_F . As a special case of a more general theorem, it is shown that for a system with zero pressure (i.e. a Fermi liquid at absolute zero) the Fermi energy E_F is equal to the average energy per particle E_0/N of the system. This result should apply both to liquid He_3 and to nuclear matter.

The theorem is used as a test on the internal consistency of the theory of Brueckner ¹⁾ for the structure of nuclear matter. It is seen that the large discrepancy between the values of E_F and E_0/N , as calculated by Brueckner and Gammel ²⁾, arises from the fact that Brueckner neglects important cluster terms contributing to the single particle energy. This neglect strongly affects the calculation of the optical potential.



N. M. Hugenholtz



L. Van Hove

Q1: Theoretical Formulism

- Starting from the Hugenholtz–Van Hove theorem that is a fundamental relation among the Fermi energy, the average energy per particle E and the pressure of the system P at the absolute temperature of zero.

$$t(k_F^n) + U_n(\rho, \delta, k_F^n) = \frac{\partial \xi}{\partial \rho_n},$$

$$t(k_F^p) + U_p(\rho, \delta, k_F^p) = \frac{\partial \xi}{\partial \rho_p},$$

The nucleon single-particle potentials can be expanded as a power series

$$\begin{aligned} U_\tau(\rho, \delta, k) &= U_0(\rho, k) + \sum_{i=1,2,3,\dots} U_{\text{sym},i}(\rho, k)(\tau\delta)^i \\ &= \boxed{U_0(\rho, k) + U_{\text{sym},1}(\rho, k)(\tau\delta)} + U_{\text{sym},2}(k)(\tau\delta)^2 + \dots \end{aligned}$$

isoscalar isovector (Lane potential)

$$\begin{aligned}
& [t(k_F^n) - t(k_F^p)] + [U_n(\rho, \delta, k_F^n) - U_p(\rho, \delta, k_F^p)] \\
&= \sum_{i=1,2,3,\dots} \frac{1}{i!} \frac{\partial^i [t(k) + U_0(\rho, k)]}{\partial k^i} \Big|_{k_F} k_F^i \\
&\quad \times \left[\left(\sum_{j=1,2,3,\dots} F(j) \delta^j \right)^i - \left(\sum_{j=1,2,3,\dots} F(j) (-\delta)^j \right)^i \right] \\
&\quad + \sum_{l=1,2,3,\dots} U_{\text{sym},l}(\rho, k_F) [\delta^l - (-\delta)^l] + \sum_{l=1,2,3,\dots} \sum_{i=1,2,3,\dots} \frac{1}{i!} \frac{\partial^i U_{\text{sym},l}(\rho, k)}{\partial k^i} \Big|_{k_F} k_F^i \\
&\quad \times \left[\left(\sum_{j=1,2,3,\dots} F(j) \delta^j \right)^i \delta^l - \left(\sum_{j=1,2,3,\dots} F(j) (-\delta)^j \right)^i (-\delta)^l \right] \\
&= \left[\frac{2}{3} \frac{\partial [t(k) + U_0(\rho, k)]}{\partial k} \Big|_{k_F} k_F + 2U_{\text{sym},1}(\rho, k_F) \right] \delta + \dots,
\end{aligned}$$

Xu et. al, Phys. Rev. C 82, 054607 (2010)

Xu et. al, Phys. Rev. C 81, 064612 (2010)

Xu et. al, Phys. Rev. C 81, 044603 (2010)

Xu et. al, Nucl. Phys. A 865, 1 (2011)

Xu et. al, Nucl. Phys. A 913 (2013) 236

Xu et. al, Eur. Phys. J. A 50 (2014) 21

Xu et.al, Phys. Rev. C 90, 064310 (2014)

Theoretical Formulism

$$\begin{aligned}\frac{\partial \xi}{\partial \rho_n} - \frac{\partial \xi}{\partial \rho_p} &= \frac{2}{\rho} \frac{\partial \xi}{\partial \delta} = \sum_{i=2,4,6,\dots} 2i E_{\text{sym},i}(\rho) \delta^{i-1} \\ &= 4E_{\text{sym},2}(\rho)\delta + 8E_{\text{sym},4}(\rho)\delta^3 + 12E_{\text{sym},6}(\rho)\delta^5 + \dots\end{aligned}$$

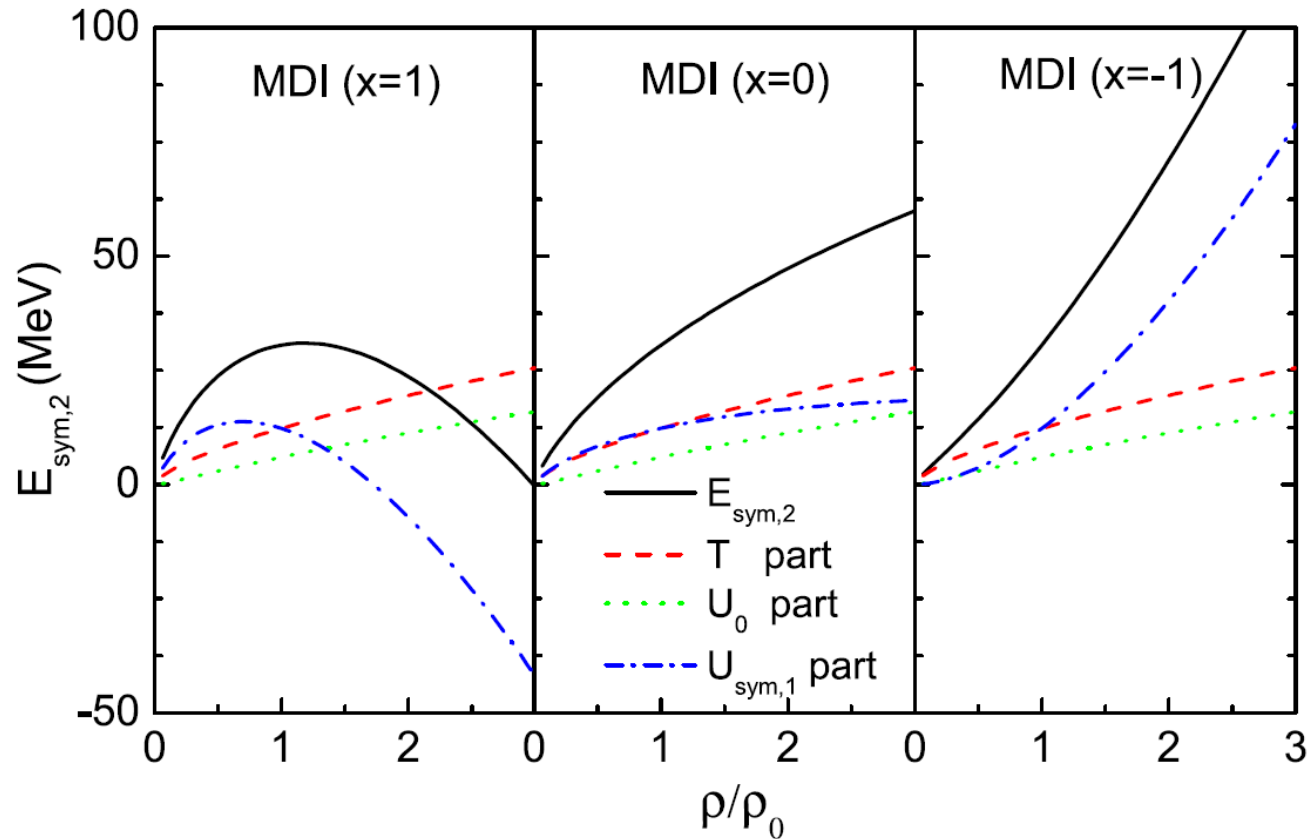
Comparing the coefficient of each term then gives the symmetry energy of any order

$$\begin{aligned}E_{\text{sym},2}(\rho) &= \frac{1}{6} \frac{\partial [t(k) + U_0(\rho, k)]}{\partial k} \Big|_{k_F} + \frac{1}{2} U_{\text{sym},1}(\rho, k_F) \\ &= \frac{1}{3} t(k_F) + \frac{1}{6} \frac{\partial U_0}{\partial k} \Big|_{k_F} + \frac{1}{2} U_{\text{sym},1}(\rho, k_F)\end{aligned}$$

Symmetry energy: kinetic energy part

isoscalar potential part + isovector potential part (most uncertain)

Connections between the symmetry energy and isoscalar and isovector parts of single-particle potential is explicitly shown.



BUU: The Momentum dependent Interaction (MDI)

Theoretical Formalism

The quadratic term $E_{\text{sym},2}$ is the most important.

$$E_{\text{sym},4}(\rho) = \left[\begin{aligned} & \frac{5}{324} \frac{\partial[t(k) + U_0(\rho, k)]}{\partial k} \Big|_{k_F} k_F \\ & - \frac{1}{108} \frac{\partial^2[t(k) + U_0(\rho, k)]}{\partial k^2} \Big|_{k_F} k_F^2 + \frac{1}{648} \frac{\partial^3[t(k) + U_0(\rho, k)]}{\partial k^3} \Big|_{k_F} k_F^3 \\ & - \frac{1}{36} \frac{\partial U_{\text{sym},1}(\rho, k)}{\partial k} \Big|_{k_F} k_F + \frac{1}{72} \frac{\partial^2 U_{\text{sym},1}(\rho, k)}{\partial k^2} \Big|_{k_F} k_F^2 \\ & + \frac{1}{12} \frac{\partial U_{\text{sym},2}(\rho, k)}{\partial k} \Big|_{k_F} k_F + \frac{1}{4} U_{\text{sym},3}(\rho, k_F) \end{aligned} \right].$$

Microscopic calculations : higher-order terms are usually negligible, less than 1 MeV at ρ_0 .

At supra-saturation densities : modify the proton fraction in neutron stars and the cooling mechanism of proto-neutron stars

Density slope of symmetry energy

The symmetry energy can be characterized by using the value of $E_{\text{sym}}(\rho_0)$ and the slope parameter L

$$L = 3\rho_0 \left. \frac{dE_{\text{sym}}(\rho)}{d\rho} \right|_{\rho=\rho_0}$$

**Density
dependence**

L: important for : the size of the neutron skin in heavy nuclei , location of the neutron drip line ,core-crust transition density and gravitational binding energy of neutron stars

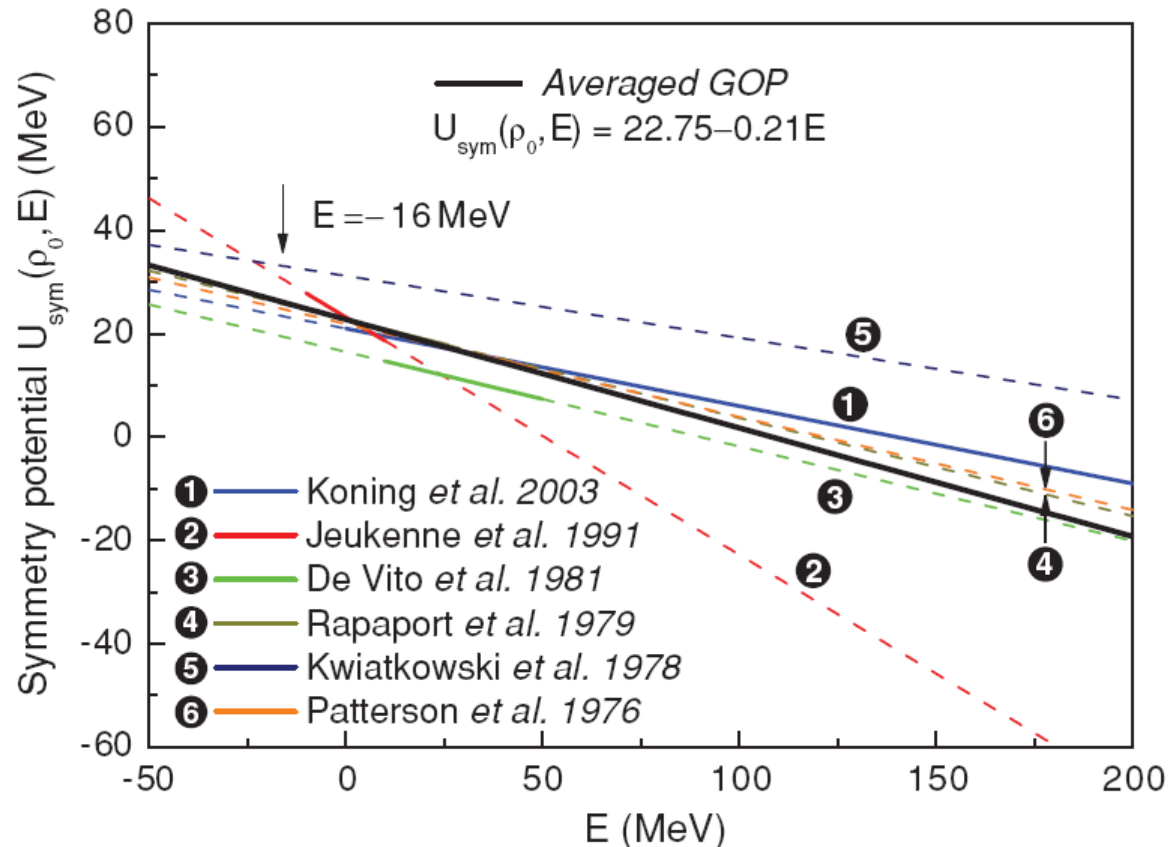
$$L(\rho) = \frac{2}{3} \frac{\hbar^2 k_F^2}{2m_0^*} + \frac{3}{2} U_{\text{sym}}(\rho, k_F) + \left. \frac{\partial U_{\text{sym}}}{\partial k} \right|_{k_F}$$

**Momentum
dependence**

Q2: Symmetry energy and its slope at saturation density

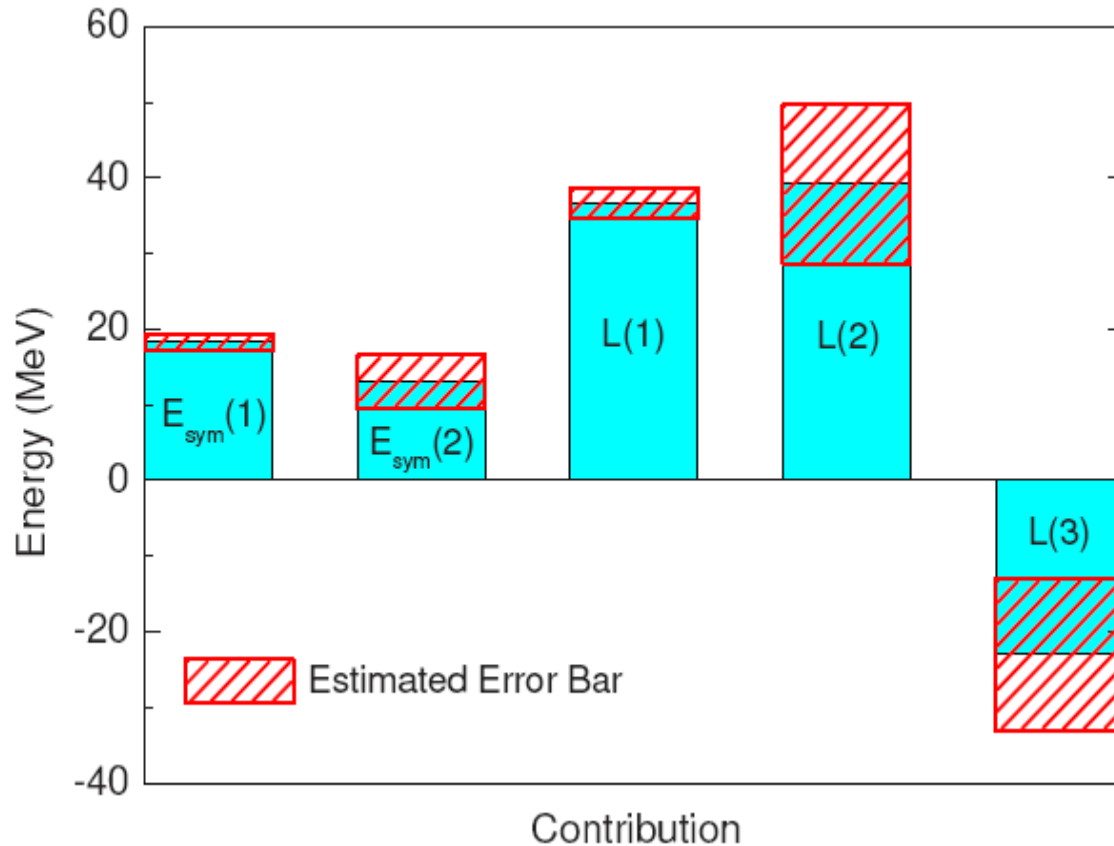
Systematics based on world data accumulated since 1969:

- (1) Single particle energy levels from pick-up and stripping reaction
- (2) Neutron and proton scattering on the same target at about the same energy
- (3) Proton scattering on isotopes of the same element
- (4) (p,n) charge exchange reactions



Constraining the symmetry energy near saturation density using global nucleon optical potentials

C. Xu, B.A. Li and L.W. Chen, PRC 82, 054606 (2010).



$$E_{sym}(\rho_0) = 31.3 \text{ MeV} \pm 4.5 \text{ MeV}$$

$$L(\rho_0) = 52.7 \text{ MeV} \pm 22.5 \text{ MeV}$$

Q3: Symmetry energy at supra-saturation density

- Some indications of a supersoft E_{sym} at high densities have been obtained from analyzing the π^+/π^- ratio data.
- Experiments have now been planned to investigate the high-density behavior of the E_{sym} at the CSR in China, GSI in Germany, MSU in the United States, and RIKEN in Japan.
- Possible physical origins of the very uncertain E_{sym} at supra-saturation densities?

$$U_0 = \frac{U_n + U_p}{2} = \frac{3}{4}u_{T1} + \frac{1}{4}u_{T0}$$

$$U_{\text{sym}} = \frac{U_n - U_p}{2\delta} = \frac{1}{4}u_{T1} - \frac{1}{4}u_{T0}$$

Effects of the spin-isospin dependent three-body force

U_0 : relatively well determined

U_{sym} : isosinglet vs isotriplet channels,

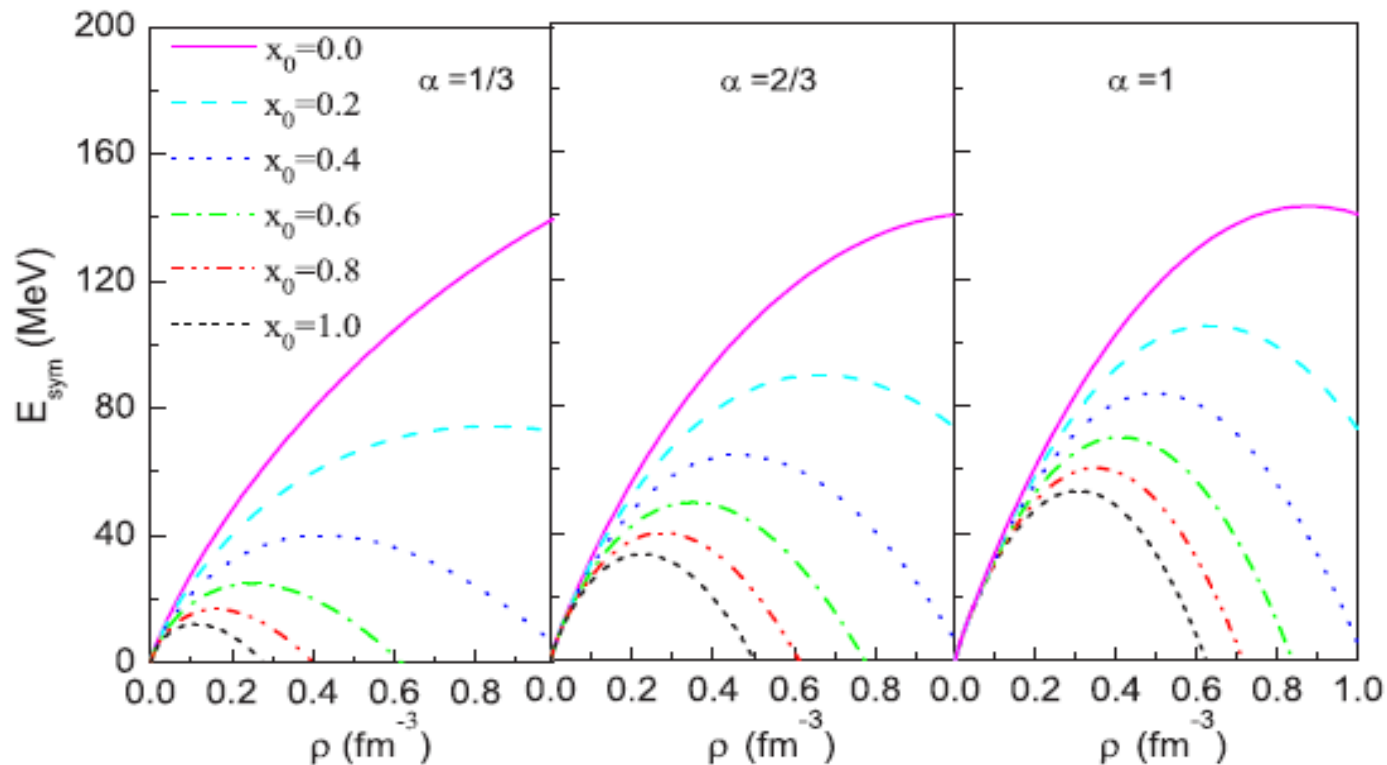
However, the U_{sym} is very poorly known especially at high momenta.

Effects of the in-medium tensor force and nucleon correlation

Effects of the spin-isospin dependent three-body force

Symmetry energy with different spin dependence x_0 and density dependence α in the three-body force (Gogny force)

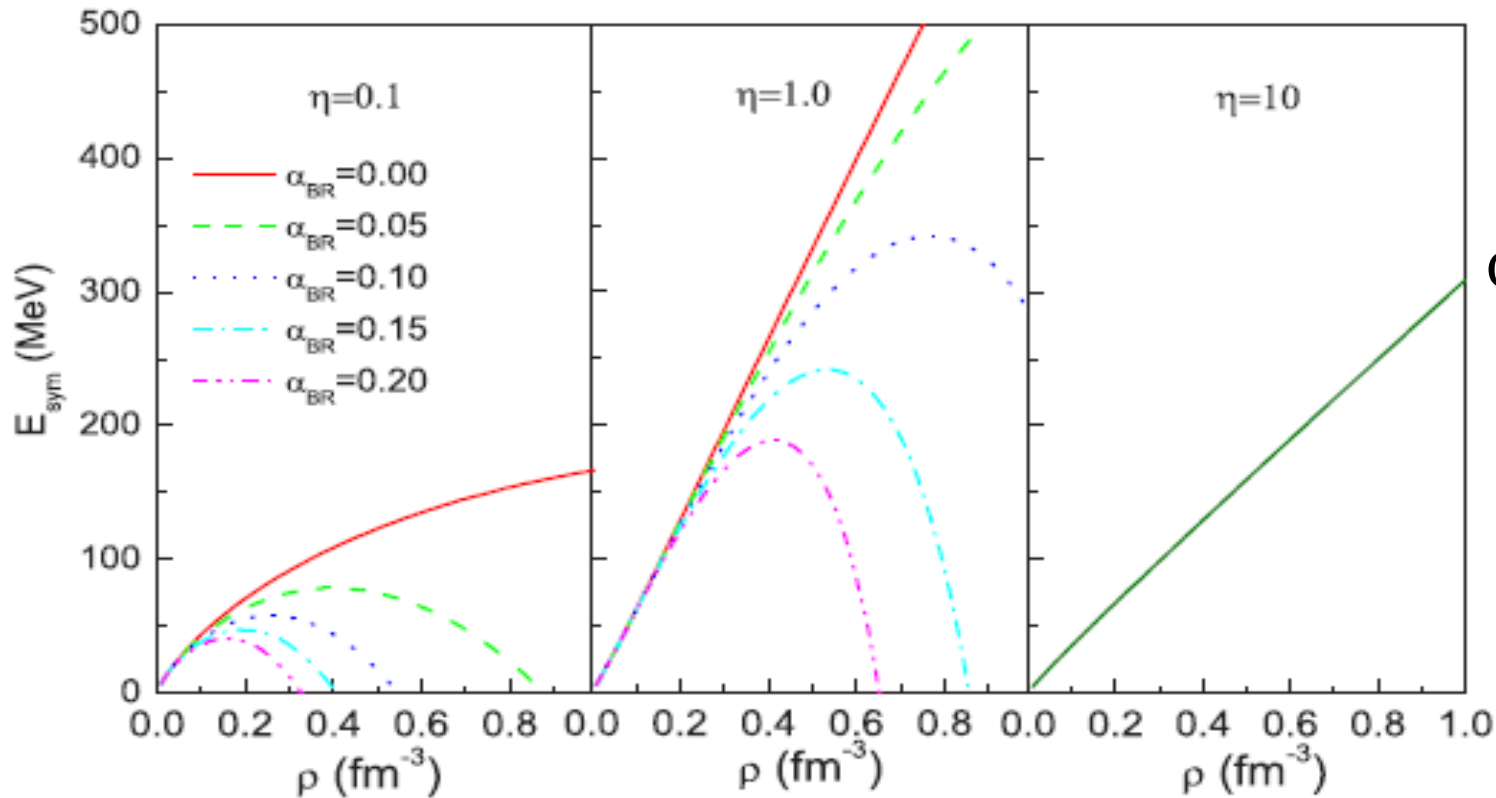
$$V_d = t_0(1 + x_0 P_\sigma) \rho^\alpha \delta(r)$$



Qualitative analysis

Effects of short-range correlations induced by tensor force

Symmetry energy with different values of the BRS parameter $\alpha_{BR} = 0, 0.05, 0.10, 0.15, 0.20$ using different values for the tensor correlation parameter.



Qualitative analysis

3. Symmetry energy and density slope extracted from cluster radioactivity

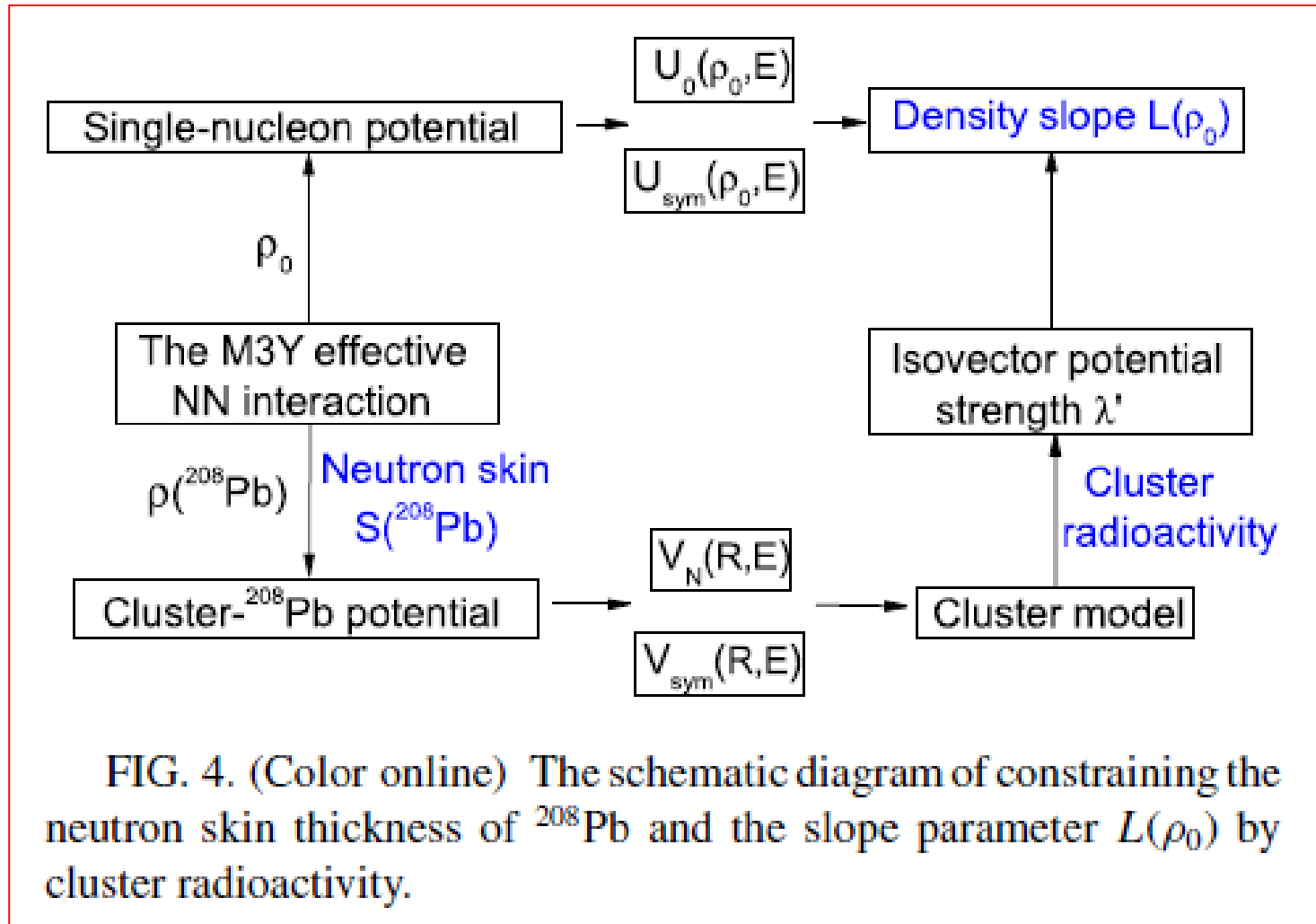


FIG. 4. (Color online) The schematic diagram of constraining the neutron skin thickness of ^{208}Pb and the slope parameter $L(\rho_0)$ by cluster radioactivity.

1. Single-nucleon potential: constrained by reaction data

$$U_{n/p}(\rho_n, \rho_p, E) = \int d\mathbf{r} [\lambda g_{00}(s, E)(\rho_n + \rho_p) \pm \lambda' g_{01}(s, E)(\rho_n - \rho_p)],$$

2. Cluster-core potential: constrained by radioactivity data

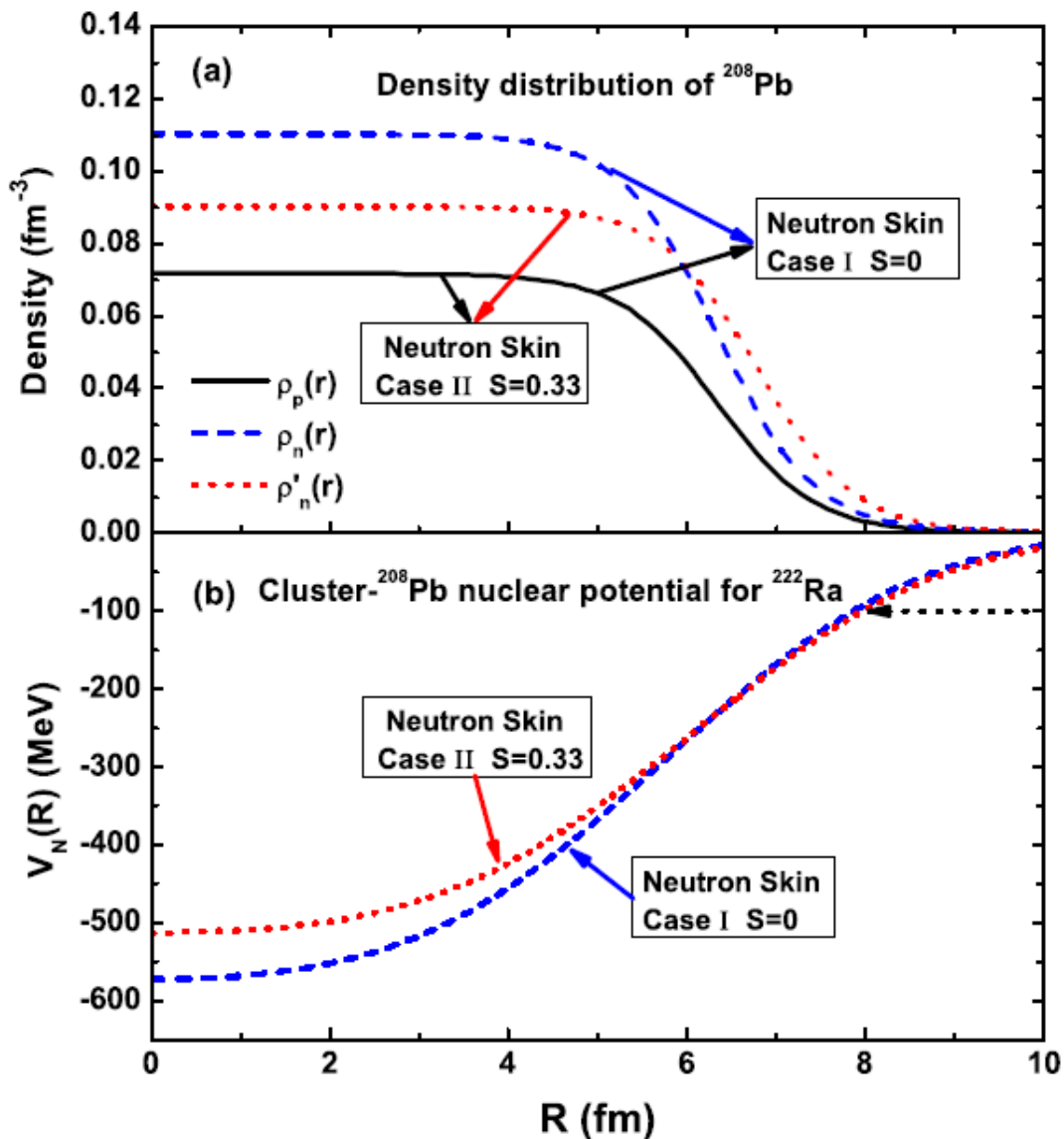
$$V_N(R) = \lambda \int d\mathbf{r}_1 d\mathbf{r}_2 (\rho_{1n} + \rho_{1p})(\rho_{2n} + \rho_{2p}) g_{00}(s, E)$$

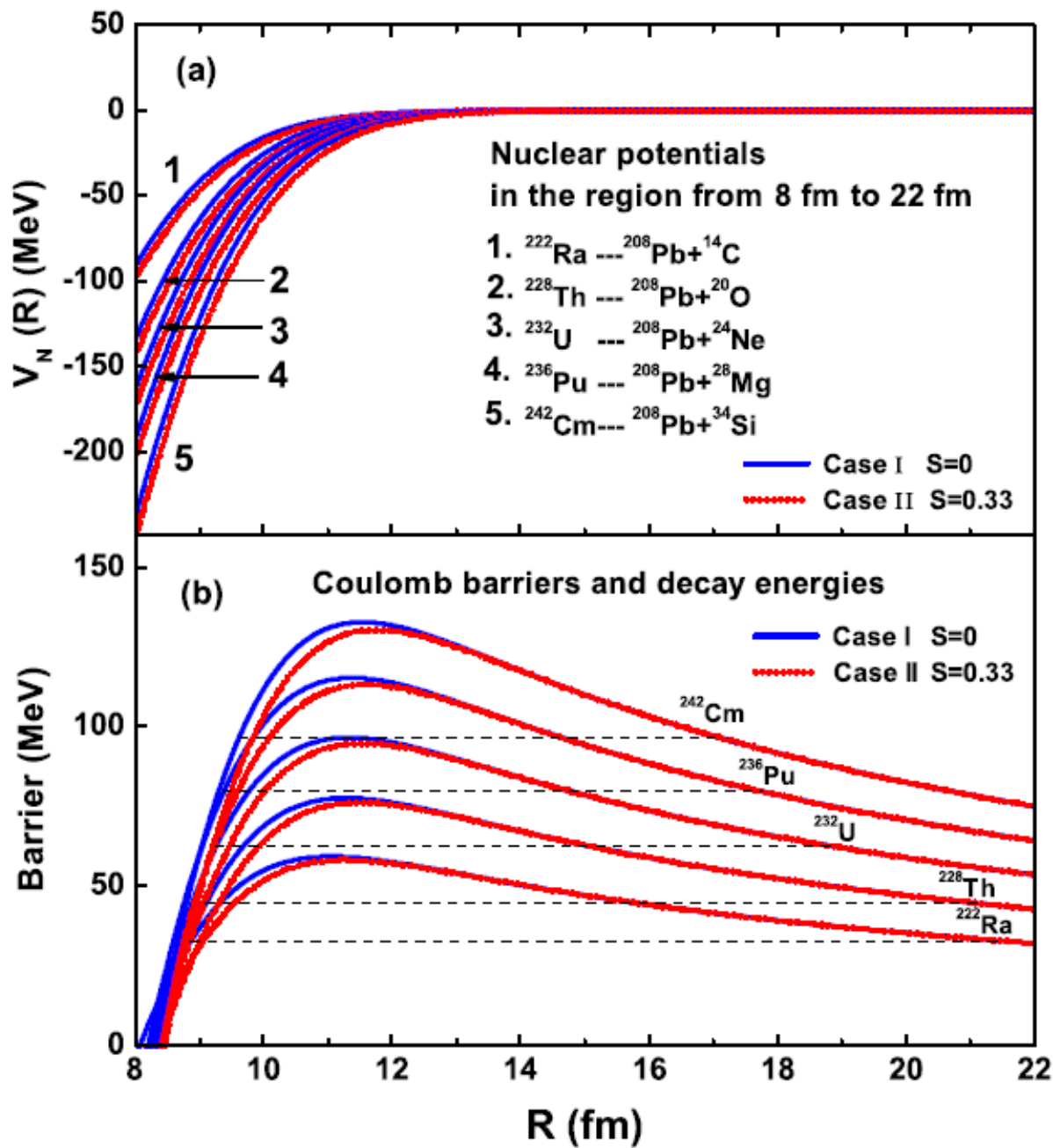
$$V_{\text{sym}}(R) = \lambda' \int d\mathbf{r}_1 d\mathbf{r}_2 (\rho_{1n} - \rho_{1p})(\rho_{2n} - \rho_{2p}) g_{01}(s, E)$$

3. Density slope of symmetry energy

$$L(\rho_0) = \frac{2}{3} \frac{\hbar^2 k_F^2}{2m} \frac{1}{1 - 1.38\lambda\rho_0} + \lambda' \rho_0 \left[\frac{3}{2} \left(214.43 + \frac{480.69\lambda\rho_0}{1 - 1.38\lambda\rho_0} \right) - \frac{7}{2} \left(1.14 + \frac{1.57\lambda\rho_0}{1 - 1.38\lambda\rho_0} \right) \frac{\hbar^2 k_F^2}{2m} \right],$$

Decay





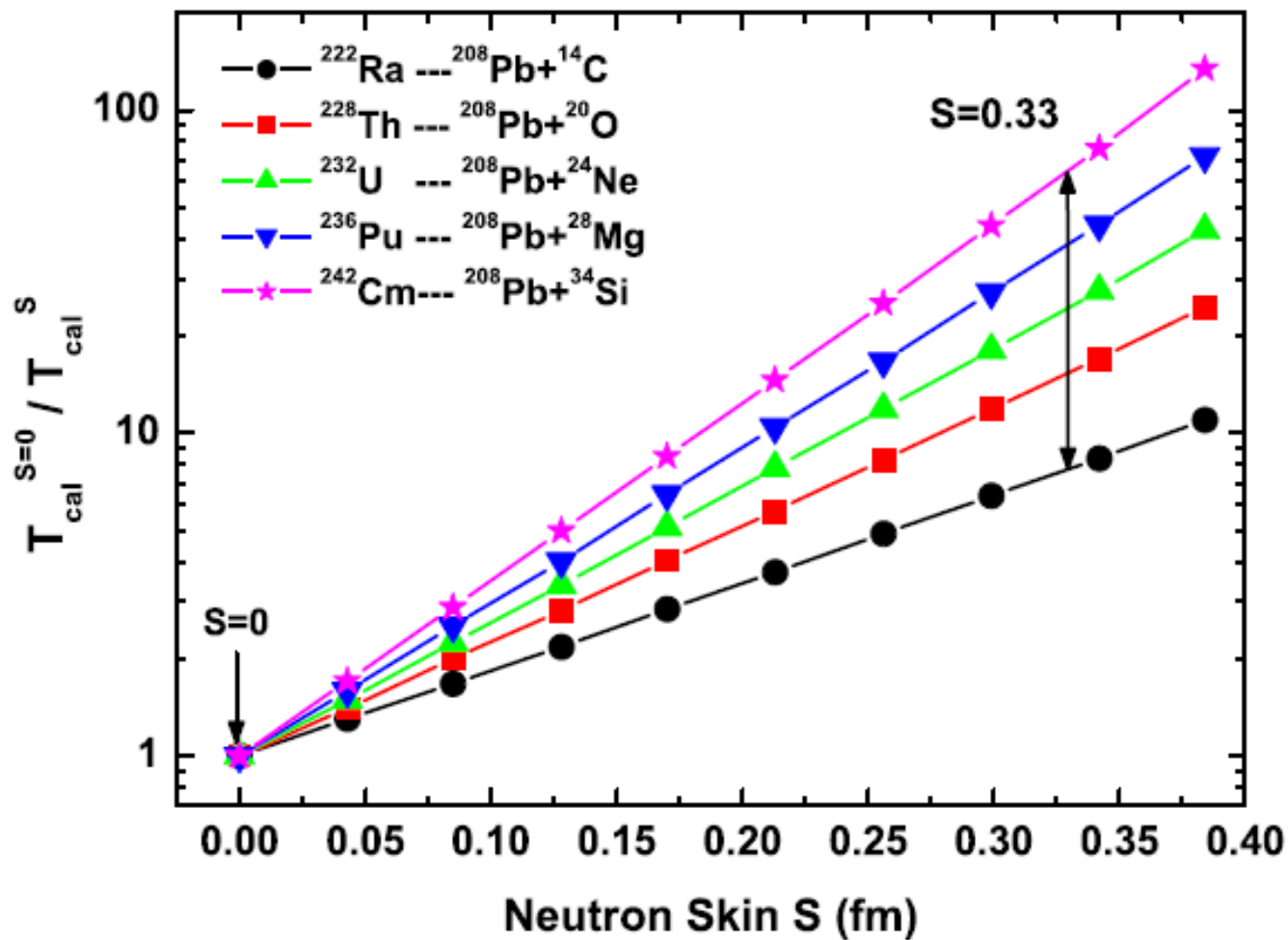
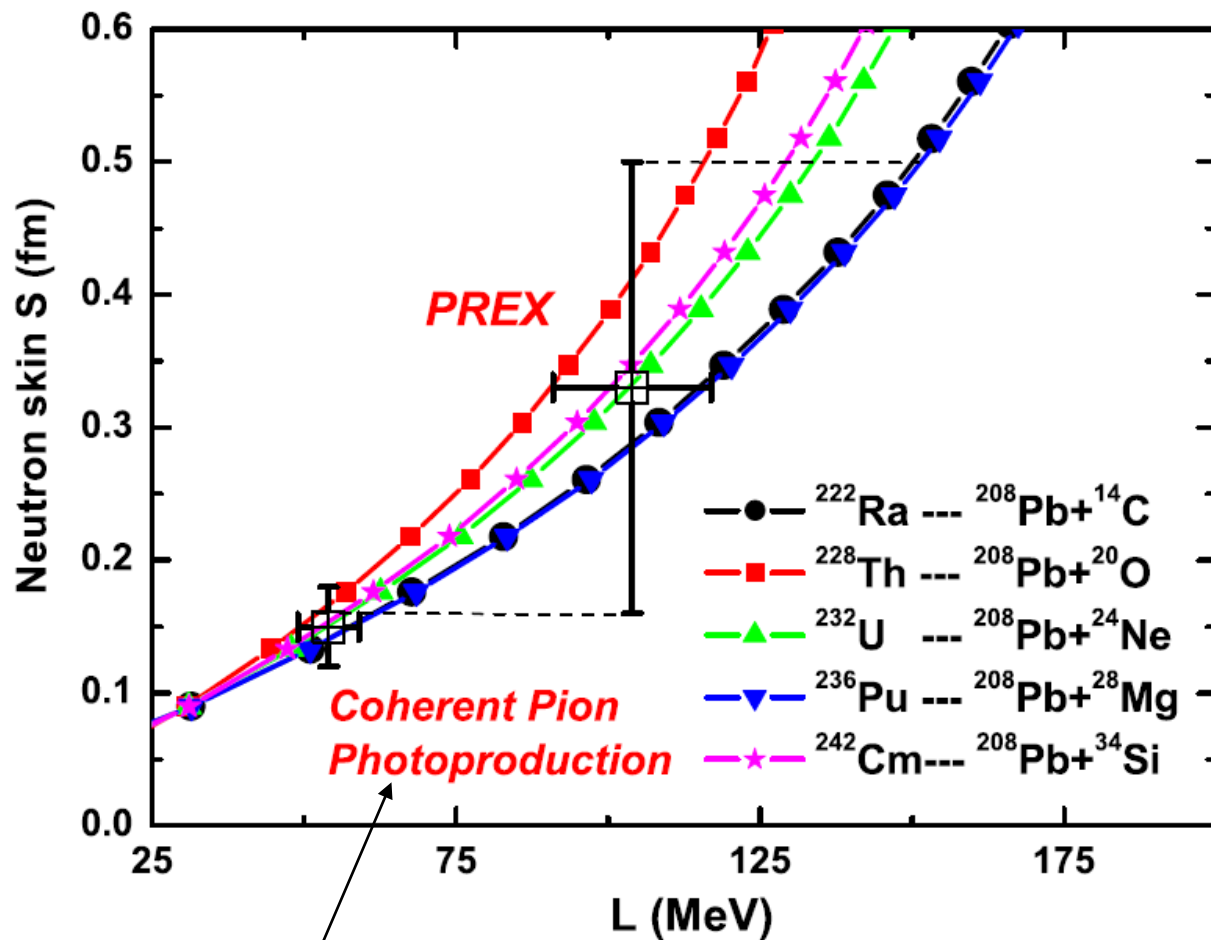


FIG. 3. (Color online) The variation of cluster radioactivity half-lives of ^{222}Ra , ^{228}Th , ^{232}U , ^{236}Pu , and ^{242}Cm as a function of the neutron skin thickness of ^{208}Pb .

Density slope of symmetry energy extracted from cluster radioactivity



$$L(\rho_0) = 54 \pm 6 \text{ MeV.}$$

Summary

General expressions are derived for E_{sym} and L by using the HVH theorem.

$$E_{\text{sym}}(\rho) = \frac{1}{3} \frac{\hbar^2 k_F^2}{2m_0^*} + \frac{1}{2} U_{\text{sym}}(\rho, k_F),$$
$$L(\rho) = \frac{2}{3} \frac{\hbar^2 k_F^2}{2m_0^*} + \frac{3}{2} U_{\text{sym}}(\rho, k_F) + \left. \frac{\partial U_{\text{sym}}}{\partial k} \right|_{k_F}.$$

E_{sym} and L at normal density: **extracted from the global optical potential [reaction data]**

$$E_{\text{sym}}(\rho_0) = 31.3 \text{ MeV}, \text{ and } L(\rho_0) = 52.7 \text{ MeV}.$$

E_{sym} and L at normal density: **cluster radioactivity [decay data]**

$$L(\rho_0) = 54 \pm 6 \text{ MeV}.$$

• **Thanks!**